3D thermography in non-destructive testing of composite structures

2016 Meas. Sci. Technol. 27 124006

(http://iopscience.iop.org/0957-0233/27/12/124006)

IOP Publishing Measurement Science and Technology
Meas. Sci. Technol. **27** (2016) 124006 (12pp) doi:10.1088/0957-0233/27/12/124006

3D thermography in non-destructive testing of composite structures

Piotr Hellstein[1] **and Mariusz Szwedo**[2]

[1] AGH University of Science and Technology, Mickiewicza 30 Ave., 30-059 Krakow, Poland
[2] MONIT SHM, Lublanska 34, 31-476 Krakow, Poland

E-mail: hell@agh.edu.pl and mszwedo@monitshm.pl

Received 25 February 2016, revised 8 August 2016
Accepted for publication 16 August 2016
Published 19 October 2016

Abstract

The combination of 3D scanners and infrared cameras has lead to the introduction of 3D thermography. Such analysis produces results in the form of three-dimensional thermograms, where the temperatures are mapped on a 3D model reconstruction of the inspected object. All work in the field of 3D thermography focused on its utility in passive thermography inspections. The authors propose a new real-time 3D temperature mapping method, which for the first time can be applied to active thermography analyses. All steps required to utilise 3D thermography are discussed, starting from acquisition of three-dimensional and infrared data, going through image processing and scene reconstruction, finishing with thermal projection and ray-tracing visualisation techniques. The application of the developed method was tested during diagnosis of several industrial composite structures—boats, planes and wind turbine blades.

Keywords: active thermography, 3D temperature mapping, non-destructive testing, data visualisation, GPU rendering, pulsed thermography, 3D thermography

(Some figures may appear in colour only in the online journal)

1. Introduction

With the growing popularity of composite structures it has become important to develop fast and accurate diagnostic methods for their inspection [1, 2]. Composite materials are typically used for large structures, where weight and durability play a key role. The preparation of composite materials is not an automated process and requires human interaction. Because of that, the quality of the resultant product varies a lot, and may contain numerous kinds of defects, such as delaminations, voids, cracks, non-uniform layer composition and other. Composites are usually inspected with non-destructive methods, which do not modify or destroy the structure during the measurement. One group of such methods is active thermography. The result of thermography measurements are thermograms—series of images, which register thermal radiation of the inspected object.

With the lowering size and cost of 3D scanners it has been become increasingly popular to use them in a variety of measurement systems. Three-dimensional scanners are mainly used as an extension to existing diagnostic systems, by including information about the dimensions and size of the inspected object. 3D scanners have already been introduced to thermography analyses, they are mainly used in medical fields, building inspections and energy auditing [3, 4]. The combination of infrared data with geometrical information allows for better visualisation of the registered thermogram and its precise localisation on an inspected object. Several infrared systems have been presented in the past few years, which allow us to perform mapping of thermal information on a 3D model. Unfortunately most of them suffer from constraints regarding the size of the inspected object. Furthermore, they are only limited to passive thermography.

This paper introduces a novel approach to 3D thermal mapping, which for the first time uses it for active thermography measurements. The difficulty of such application comes from the fact that such analyses register thermograms, which vary in time. This required a new thermal mapping method, which maps temperatures using ray-tracing GPU rendering algorithms. The mapping is being performed in real-time during image viewing. This allows the user to perform different kinds

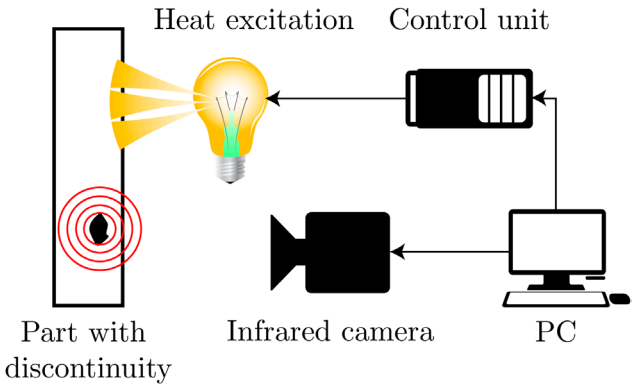

Figure 1. Pulsed thermography measurement principle.

of processing algorithms on an analysed image and observe a live update on a 3D model of the inspected structure.

The proposed measurement system uses classical step pulse thermography and enhances it with advanced visualisation methods. The presented solution is not limited to analysis of small areas. It has been designed especially for non-destructive diagnostics of large, industrial structures such as boats, planes and wind-turbine blades.

2. Background

2.1. Active thermography

Thermography measurements rely on the measurement of the temperature of the objects surface [5]. It has been observed, that whenever something is out of order or malfunctions, it often produces excessive heat. In mechanics this is typically the result of an unplanned friction, in electronics it can be produced by too large currents. Thermography measurements are divided into two groups—passive and active [6]. Passive thermography registers temperatures as they are, with no external energy stimulation applied by the operator. The result is typically a single image. This analysis is very popular in electronics or building inspection.

Active thermography is a non-destructive measurement method, which introduces thermal disturbance in the inspected structure, as presented in figure 1 [7]. The generated heat flow affects the surface temperature of an object, which can be observed with a thermovision camera [8]. The result is a movie, which contains a series of thermograms. There are several ways to alter the temperature of an object, each one of them requires different hardware setup and processing methods. Three main energy sources that are used in active thermography are optical excitation [9], electromagnetic excitation [10] and mechanical excitation [11]. Optical excitation is performed with the use of an external heat source, electromagnetic excitation is obtained with induced eddy currents and mechanical excitation is applied using an ultrasonic transducer. An active thermography measurement is identified not only by its excitation source, but also the way energy is applied to the structure. The energy signal may be a constant step function (as in step pulse thermography) or contain a synchronised periodic modulation (e.g. in lock-in thermography).

Because active thermography is a fast and contactless method, it is becoming widely used in non-destructive testing of composites [12]. The significant advantage of active thermography is that it is relatively simple, therefore the measurement can be performed by a trained, but non-professional worker. The actual processing and analysis of data is more complicated and requires both knowledge and experience, but it does not have to be done on-site. Typical active thermography measurement is noisy and does not produce information about the type of the defect or its depth. However that information can be obtained with the use of more advanced processing techniques, such as absolute thermal contrast method [13] or TSR [14].

2.2. 3D thermography

A 3D thermogram can be obtained by fusing an infrared image with the 3D model of the inspected object, as presented in figure 2. 3D thermography is a relatively new field, which has started with the advances made in 3D scanner technology. The simplest way to perform a 3D reconstruction, is to extract three-dimensional data from an image using stereo vision [15]. That technique uses two or more relatively calibrated cameras, which observe the same scene from many angles. This method is very limited and requires as many thermovision cameras as vision cameras to correspond the temperatures with appropriate image pixels. A more advanced technique is structure from motion (Sfm). It uses a single camera, which takes a series of images that are combined with motion signals, which allow it to estimate the camera positions of consecutive images [16].

A more complete 3D representation of an object is a point cloud [17]. It consists of a set of points in the same coordinate system. In order to obtain a three-dimensional point cloud of the observed object, it is necessary to use a 3D scanner. There are two popular ways to obtain the information about the distance to the measured object—using time of flight or triangulation methods. Time of flight 3D scanners measure the time that it takes for the emitted laser to return. Their accuracy is limited to the precision of time estimation. They can be used for measuring large distances, that is why they are very common in military and geography mapping applications. A typical time of flight 3D scanner is a LIDAR (light detection and ranging). LIDAR scanners used to be very big, heavy and expensive. As a result they were not a popular choice in mobile applications, however this has begun to change [18]. Triangulation 3D scanners use an emitter and a sensor, which are placed next to each other. An emitter projects a light pattern, which is observed by the camera sensor. By using simple trigonometry it is possible to obtain a depth map, which is a 2D image, where individual pixel values represent distances. A popular 3D scanner using triangulation method is a microsoft kinect [19]. Because of its availability and low price, it has become very popular in robotics applications.

3D scanners are often accompanied by an RGB vision sensor, which allows us to colour the acquired point cloud. The output of a thermovision camera is similarly a series of pixels with corresponding temperature values, that is why it is

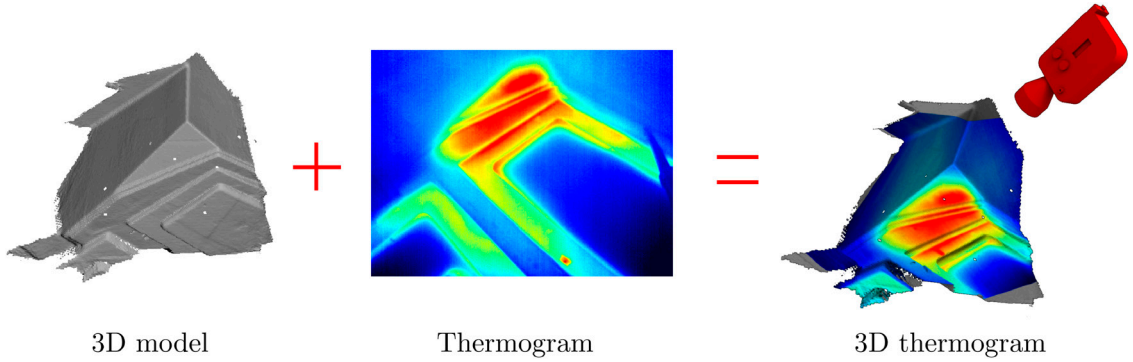

Figure 2. Construction of a 3D thermogram by combining a 3D model with an infrared image.

possible to apply similar algorithms to colour the point clouds with temperatures. Such a photogrammetry method combined with image fusion is widely popular in medicine and building inspections [20]. Construction of 3D thermograms has been studied with various three-dimensional scanning techniques available, such as Sfm [21], LIDAR scanners [22] and structured light systems [3].

An improvement over existing designs was first handheld 3D thermography system introduced by Stephan Vidas [23]. It was developed for energy auditing and required long post-processing to perform the 3D temperature mapping. However the system allowed the operator to move within a fixed volume of size around 3 m and used weighted ray casting for temperature mapping. Just recently the system has been upgraded to allow for real-time visualisation of results during the measurement [24]. This does not change the fact, that HeatWave, as well as all other existing systems, can only be used for passive thermography analyses, with temperatures that are time-independent. In active thermography it is necessary to observe the process that goes behind the temperature changes within the structure, therefore the temperatures change all the time. This requires different approach for both registration of data and its processing.

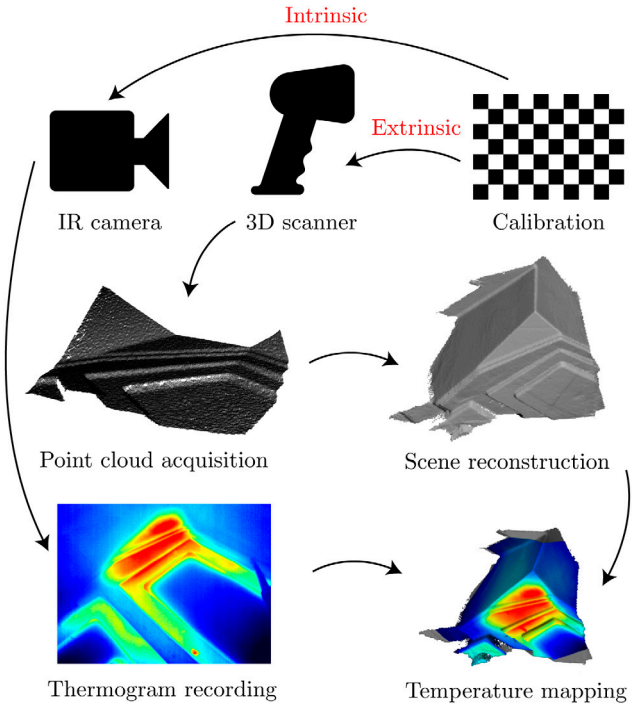

Figure 3. Steps required for temperature mapping.

3. IR3D analysis

In order to combine 3D temperature mapping with active thermography, a new analysis called *IR3D Analysis* has been developed by authors. This method is universal and may also be used for passive thermography measurements. The method requires a 3D scanner to gather information about the inspected object and later construct a three-dimensional model. During 3D model generation consecutive camera positions are estimated, therefore it is not necessary to use any additional equipment to keep track of camera orientation. The method is not limited in size to a fixed volume and is scalable. In this paper authors focus on the use of IR3D Analysis in combination with step pulse thermography technique, but it can be successfully applied to all active thermography measurements.

Because 3D thermography is a complicated, multi-modal representation, there are a number of things that have to be considered. The steps, which are required to obtain a complete 3D thermogram are presented in figure 3. First all data has to be recorded, according to a measurement procedure described in section 3.1. Then a 3D model is reconstructed, with techniques outlined in section 3.2. Finally the temperatures can be mapped on a 3D representation, as shown in section 3.3. section 4.2 focuses on the geometrical calibration of the measurement system, which is required for accurate thermal mapping.

3.1. Measurement procedure

As described in section 2.1, a pulsed thermography measurement requires to apply external heating to the structure. A single measurement consists of two phases heating and cooling—and is registered as a sequence of images. When performing a diagnostic of large composite structures, it is often necessary to perform an extensive amount of pulse-thermography measurements. The area covered by a single measurement depends on the field of view of the lens system and is typically less than 1 m^2. In order to obtain a 3D representation of a measured object, it is necessary to register depth clouds with a 3D scanner. Registration of depth clouds has to be active

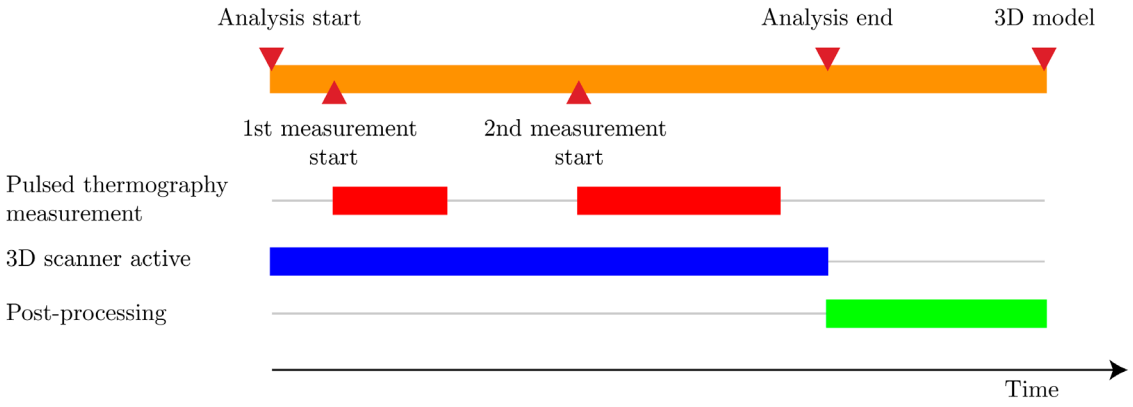

Figure 4. Measurement procedure of IR3D Analysis with puled thermography.

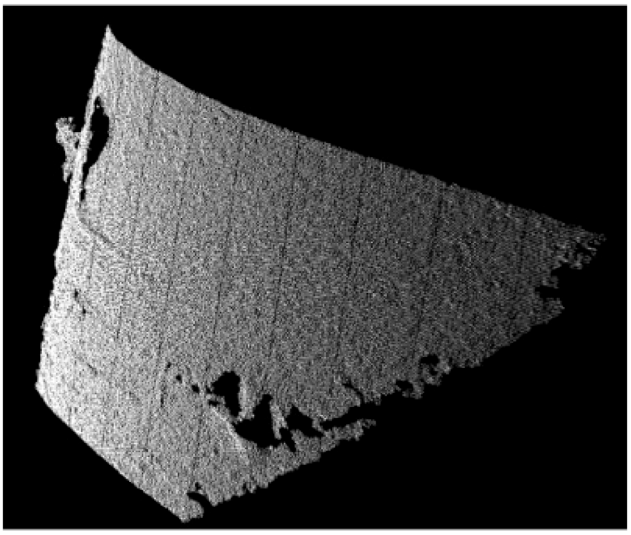

Figure 5. Registered point cloud of a part of a wind-turbine blade.

through the whole analysis—it starts before the first thermographic measurement and ends after the last one (figure 4). If only one thermographic measurement is to be made, in order to obtain a more complete 3D model it is later necessary to capture additional 3D clouds by manually pointing the scanner at the inspected structure from different angles. Even though typical 3D scanners have high range of registration, it is advisable to capture the structure with 3D scanner being no further than 3–5 m. In low-cost 3D scanners, the accuracy of depth map is dependant on the distance that is being measured and equals about 1% (1 cm error at 1 m) [25].

After the whole object has been inspected, results consist of both thermograms and depth files, with corresponding related timestamps. If accurate temperature mapping is required when the system is in motion, it is necessary to synchronise registration of both thermal camera and 3D scanner. Active thermography measurements are performed when the hardware is standing still, therefore it is not crucial to have full synchronisation.

3.2. 3D model generation

The output from a 3D scanner is a depth map. A depth map can be treated as a 2D image, where pixel values represent the distance to the object. In order to transform them into the point cloud representation, it is necessary to know the intrinsic parameters of the scanner. Such parameters are often provided by the scanner manufacturer, but in order to obtain maximum accuracy, it is advisable to perform geometrical calibration of the scanner [26]. When the camera model parameters are known, the depth values can be back projected into the three-dimensional scene to form a point cloud. Low-cost 3D scanners typically register data, which is very noisy (figure 5). This does not pose a problem, because during cloud fusion such data will be averaged and discarded.

The next step is the generation of a 3D model, with corresponding camera positions and orientations for every registered timestamp. This is performed with a cloud fusion algorithm called kinect fusion [27]. Instead of an original implementation, its open-source equivalent called Kinfu is used. Kinfu algorithm is created as a module to the point cloud library, which is a popular 2D and 3D image and point cloud processing library [28]. The fusion algorithm performs two tasks—finds the new camera transformation and fuses the registered point cloud to previously gathered data. The generated 3D model can be rendered with marching cubes algorithm [29]. It has been shown that cloud fusion using the Kinfu algorithm can operate in real-time during the acquisition of depth files, but in order to minimise the hardware requirements for the measurement system this step is performed in post-processing. 3D model generation is done only once for every analysis.

Figure 6 presents a basic three-dimensional setup, which displays the operation of cloud fusion algorithms. The scene contains two objects with multiple flat surfaces at different angles. The first image presents how the reconstructed model looks after only two frames were captured from a 3D scanner. The model contains many holes and the planes are wrinkled. The image on the right was obtained after a series of frames captured from many angles have been fed into the kinect fusion algorithm. The surfaces are smooth and the holes are closed. Furthermore there are many more details distinguishable, such as a small towel, which was placed on top of first two stairs.

The Kinect fusion algorithm uses a modified iterative closest point (ICP) algorithm for pose estimation. Since the ICP algorithm is widely used for the geometric alignment

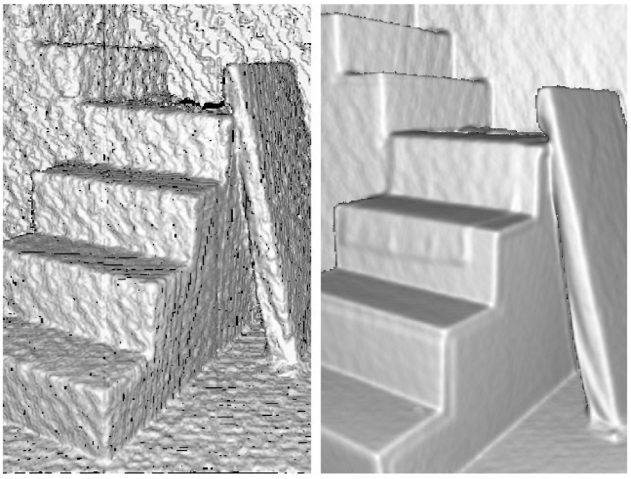

Figure 6. Fusing point clouds to smoothen the model.

of 3D point clouds, there exist many of its variations [30]. Its main principle is to find the transformation between two consecutive point clouds, which share a common group of points. Typically the algorithms searches for an alignment, in which the sum of Euclidean squared errors between estimated and registered point positions is the smallest. When a match is found, the fusion algorithm tries to merge the new point cloud into the previously gathered data. To increase the accuracy of fusion algorithm the point clouds are transformed to surface representation and stored as truncated signed distance function (TSDF). TSDF allows easy merging of new data with the use of weight averaging. Additionally this operation can be fully paralleled. This allows the whole cloud fusion algorithm to work on GPU, which greatly speeds it up.

The performance of the cloud fusion algorithm is strongly dependant on the registered point clouds. Cloud fusion works best, when the registered object has many distinctive features [31]. The most effective results are obtained, when at least two perpendicular planes are present in the scene. On the contrary, if the scene contains only one plane and the user moves in parallel motion, then the reconstruction algorithm has problems with the estimation of current camera rotation. The quality of the registered point clouds is not so important, because all noise and misalignments will be smoothed out by the fusion. During the point cloud registration, it is important that the scene is a rigid body and does not change throughout the analysis. When an object is removed from the scene during analysis, the cloud fusion averaging algorithm will eventually also discard it from the 3D model.

The original Kinfu algorithm has limitations regarding the volume within which the cloud fusion can be performed, which is around $3 \times 3 \times 3$ m, depending on the required resolution. To overcome this, an alternative algorithm called KinfuLargeScale has been used, which does not restrict the user to specific registration volume [32]. The scene reconstruction is still performed in a fixed volume, but whenever the user moves by the distance larger than half of the volume, the registration volume is shifted. Previously fused data is not discarded and is later used to generate the full world model. KinfuLargeScale allows us to measure much

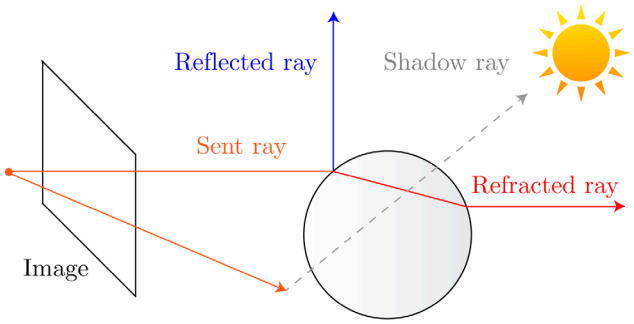

Figure 7. Ray tracing algorithm principle.

larger constructions which are typically diagnosed with active thermography, such as boats or planes. The accuracy of 3D reconstruction for a normal volume size is around 10 mm [33].

3.3. Temperature mapping

The usage of active thermography requires the temperature mapping to operate in real-time. Every area that is inspected has a corresponding thermographic sequence, which consists of many thermograms. One of the requirements of the presented method is to allow the user to move to any specific file and frame of the whole analysis and immediately observe on the 3D model where it was performed and how are the recorded apparent temperatures distributed. Additionally, the user has to have the ability to apply processing algorithms on the thermogram and observe live update on the 3D representation. Finally the temperature mapping has to be able to work with thermographic systems equipped with wide-angle lenses, which introduce huge distortions.

The above requirements can be met using a ray-tracing technique (figure 7). Ray-tracing is a rendering method in which an image is created from a series of light rays, which are traced through the scene. When a ray hits an object, several phenomena's, such as reflection and refraction, are considered. The ray-tracing method allows us to closely represent the way light moves in reality. The output images are often physically accurate. The huge advantage of ray-tracing rendering is the possibility to fully modify the path of every single ray in the scene. This allows us to simulate image distortions, which are the result of lens optics. A camera model defined in a ray-tracing rendering engine can simulate not only radial and tangential distortions, but also other effects such as chromatic aberrations. The main disadvantage of the ray-tracing method is it's slow speed, which makes it almost impossible to adapt it to real-time visualisation. Fortunately in the recent years ray-tracing calculations have been successfully moved to GPU, which allow them to operate at a much larger speed than before [34].

To make the data visualisation and temperature mapping as fast and fluid as possible, a special real-time GPU renderer has been created. The ray-tracing rendering engine is based on SmallLuxGPU (SLG), which is a part of LuxRender open source physically based renderer [35]. LuxRender has its origins in PBRT, a well structured and fully documented

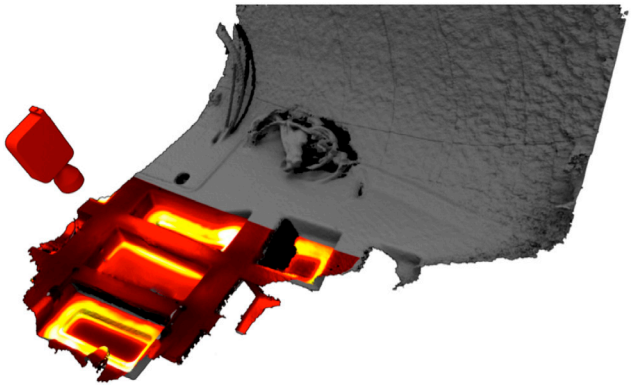

Figure 8. Temperatures mapped on a boats hull model.

ray-tracing engine [36]. SmallLuxGPU allows the user to easily render a scene, which consists of several objects and light sources, with real-time performance. High level API gives the possibility to modify elements and parameters on the fly and quickly restart rendering with new scene settings. The user has full control of the camera observing the scene and may freely move it. Because SLG is a physically accurate renderer, every defined object needs to have material specified, which contains a series of parameters, such as its roughness, diffuse reflection, absorption, etc.

In order to map temperatures on a 3D model, a unique method has been proposed. In SLG renderer, the colour of a pixel is determined by the light that enters the virtual camera. Every object, which is visible on the final image, needs to reflect light in the direction of the observer. The amount of light reflected is described by Bidirectional reflectance distribution function (BRDF) and is proportional to the surfaces irradiance at a point. The total irradiance at a point is a sum of incident radiances coming from all light sources present in the scene. SLG allows to create a variety of different light types, such as a point light, a spot light, an area light, an environmental light and a projection light.

The ProjectionLight available in SLG is particularly useful, as its behaviour imitates a normal, real-life projector. Using ProjectionLight it is possible to project an image file to the scene. Unfortunately, the light uses perspective projection, which can only be defined by specifying its field of view. Because of that limitation, a new light called CameraLight has been designed by authors, which replaces a simple projection with ability to fully declare the camera model of the lens system. A complete formula can be obtained by combining intrinsic and extrinsic camera parameters, as shown in equation (1).

$$\begin{bmatrix} x \\ y \\ z \end{bmatrix} = C \cdot P \cdot \begin{bmatrix} U \\ V \\ W \end{bmatrix} = C \cdot \begin{bmatrix} X \\ Y \\ Z \end{bmatrix} \tag{1}$$

Here world coordinates (U,V,W) are transformed to the camera coordinates (X,Y,Z), using transformation matrix P. Then camera coordinates are converted to film coordinates (x,y,z), using camera matrix C. This projection transformation is often defined as a 4×4 camera matrix in homogeneous coordinates. The full projection can be further transformed to form equation (2).

$$\begin{bmatrix} x \\ y \\ z \end{bmatrix} = \begin{bmatrix} f_x & 0 & c_x \\ 0 & f_y & c_y \\ 0 & 0 & 1 \end{bmatrix} \cdot \begin{bmatrix} r_{11} & r_{12} & r_{13} & t_1 \\ r_{21} & r_{22} & r_{23} & t_2 \\ r_{31} & r_{32} & r_{33} & t_3 \end{bmatrix} \cdot \begin{bmatrix} X \\ Y \\ Z \end{bmatrix} \tag{2}$$

Here camera matrix C is described using camera focal lengths (f_x,f_y) and principle points (c_x, c_y), which represent the optical centres. The transformation matrix P is defined by rotation and translation parameters.

In order to take into consideration the radial and tangential distortions of the system, a rational function (RF) model is used [37]. The RF model was designed especially for wide-angle lenses, but can be used to successfully simulate any lens geometry. The correction of pixel values is modelled using additional parameters obtained from calibration.

The correction of radial distortions is presented in (3) and (4).

$$x_{\text{corrected}} = x \cdot \frac{1 + k_1 r^2 + k_2 r^4 + k_3 r^6}{1 + k_4 r^2 + k_5 r^4 + k_6 r^6} \tag{3}$$

$$y_{\text{corrected}} = y \cdot \frac{1 + k_1 r^2 + k_2 r^4 + k_3 r^6}{1 + k_4 r^2 + k_5 r^4 + k_6 r^6} \tag{4}$$

The tangential distortions can be corrected using (5) and (6).

$$x_{\text{corrected}} = x + [2p_1 xy + p_2(r^2 + 2x^2)] \tag{5}$$

$$y_{\text{corrected}} = y + [p_1(r^2 + 2y^2) + 2p_2 xy] \tag{6}$$

In equations (3)–(6), r is the distance between the original coordinate and the image center. The parameters defining all distortion coefficients are typically provided in the form of a horizontal matrix, shown in (7). A complete set of intrinsic camera parameters consists of both camera matrix and distortion coefficients.

$$K = \begin{bmatrix} k_1 & k_2 & p_1 & p_2 & k_3 & k_4 & k_5 & k_6 \end{bmatrix} \tag{7}$$

By using the ray tracing rendering method, each camera pixel can be altered individually. The presented camera light model allows us to take into consideration the distortions of thermographic camera, that have to be removed, before mapping the temperatures on the fused 3D model (figure 8).

4. Measurement system

In order to verify the functionality of the presented method, authors have prepared a dedicated step pulse thermography measurement system. This is just one exemplary implementation of the IR3D Analysis method, because it may be used with all passive and active thermography measurements setups.

4.1. Hardware

The developed hardware system is based on the typical long pulse thermography setup and contains an infrared camera with two halogen lamps that heat the inspected structure (figure 9).

Figure 9. IR3D Analysis hardware.

The lamps are fully programmable via a controller, which can modify their heating power and modulation frequency. A 3D scanner is attached directly to the infrared camera with a specially manufactured frame. At the bottom an RGB sensor is mounted, which captures standard coloured images of the observed scene. All hardware is closed in a metal casing and can be easily mounted on a camera tripod.

A FLIR A300 infrared camera has been used, with 320×280 pixel resolution and 3 Hz maximum acquisition rate. Because the system is intended to be used in the inspection of large constructions, the camera has been equipped with a 4 mm fish-eye lens, which increases its field of view from $25° \times 18.8°$ to $90° \times 73°$. This results in fewer images that need to be registered to cover the whole inspected object, but also introduces large distortions. For accurate temperature mapping, it is necessary to reduce all distortions with proper geometrical calibration of the lens system.

The 3D scanner is a structure IO sensor, that is especially designed for mobile applications [38]. The device uses triangulation principle described in section 2.2, to obtain a three-dimensional point cloud of the scanned object. The scanner is powered from a USB port, it is very light (95 g) and has small dimensions (119.2 mm × 27.9 mm × 29 mm), which makes it ideal for mobile diagnostic purposes. Many commercially available scanners cannot be placed closer than 80 cm from the structure. In active thermography it is desirable to place the system close to the structure, to increase the heating efficiency. The Structure IO minimum registration distance is 40 cm, which allows us to place the system in finest distance from the inspected object. It must be noted, that the field of view of the 3D scanner is much smaller then the infrared camera, therefore for best point cloud registration it is necessary to move farther from the inspected structure than during thermographic measurement.

4.2. Calibration

For accurate temperature mapping, it is necessary to reduce all distortions with proper geometrical calibration of the lens system. The calibration has been done on a modified Zhangs chessboard pattern method [39]. Because thermographic cameras work in an infrared spectrum, a printed calibration pattern is not visible by the detector. Many infrared calibration patterns consist of elements, which are hotter than the surroundings. For this purpose a specially developed Peltier unit matrix calibration board has been used, which was previously introduced by the authors [40]. The calibration board uses thermoelectric coolers to increase the contrast and efficiency of calibration images (figure 10). When current flows through a cooler, it transfers heat from one its side to another. This results in one side of the Peltier unit to become hot, and the other cold. As a result the pattern can be either cooled down, or heated up. This way, it can be easily identified on a recorded thermogram.

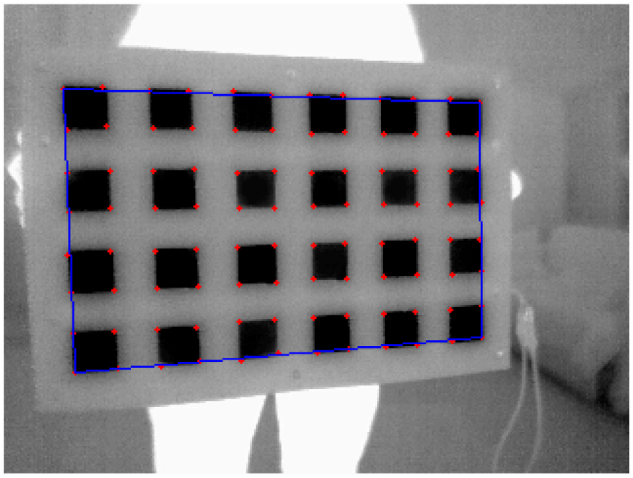

Figure 10. Peltier calibration board with cold side directed at the camera.

The calibration board consists of four layers, as presented in figure 11. At the back there is a 3 mm thick aluminium plate, which is responsible for dissipating the heat and preventing the damage of the Peltier units. The second layer is a 3 mm thick wooden frame, which holds all units. The frame has been cut out by laser and has special sockets for individual Peltier modules, as well as a path for electrical connection between them. The third layer is a 3 mm thick insulation frame, followed by a 1 mm mask layer. The role of the insulation frame is to prevent direct contact between Peltier modules and front layer, in order not to affect its temperature, which would make edge detection a much harder task. The board is 390 mm wide and 270 mm high. Because Peltier modules require current to operate, a 30 V power supply is attached at the side of the calibration board. With 24 Peltier modules mounted in series, the power supply delivers around 1.25 V for each unit. Even though the current is low, it is enough to create a temperature difference of about 20 °C between the front and back plate. The calibration board can be easily dismounted and the frame that holds thermoelectric coolers can be swapped. This allows the calibration board to create both cooled and heated pattern, depending which side of the module is directed at the camera.

Additionally to geometrical calibration of the camera, the relative calibration between the scanner and the infrared camera is necessary to perform the temperature mapping.

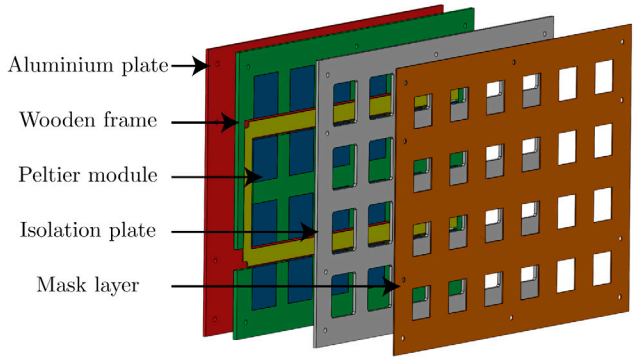

Figure 11. Exploded view of the calibration board layered design.

The calibration has been performed with the same Peltier unit matrix calibration pattern. In order to perform extrinsic calibration, it is necessary to detect the same features (keypoints) on both thermogram and depth map from several system positions. Because the calibration board has a layered construction, the Peltier modules are on different level than the front of the board. This allows the 3D scanner to extract single squares and the chessboard pattern from the registered point clouds.

4.3. System configurations

The designed system is very mobile and versatile. It can be mounted differently depending on the requirements (figure 12). There are three basic configurations in which the system can operate and has been tested:

- System is mounted on a tripod, the communication is wired. Used for normal structure inspections.
- System is mounted on robot, communication is wired. Used for diagnosis on production-line.
- System is lifted on lines and operated wirelessly. Used for wind-turbine blades inspections.

In order to allow the system to operate wirelessly, some adjustments needed to be made. Wireless communication greatly limits the amount of data that can be sent between application and hardware system. Fortunately, it is possible to connect with a FLIR camera using Wi-Fi connection. At the registration frame rate of 3 Hz the live stream does not pose a problem. However it is impossible for the 3D scanner to operate autonomously. An additional Raspberry Pi hardware has been added, which controls it and stores depth files on an external hard drive. The host computer connects with Raspberry Pi module and controls its registration process. It is important to keep full time synchronisation between the timestamps generated for 3D depth files captured on the external Raspberry Pi module and infrared files generated on host computer.

4.4. Software

All algorithms required to perform a IR3D Analysis have been created as a module to ThermoAnalysis software [41]. ThermoAnalysis is a software used for acquisition and analysis of infrared images. The images (or videos) can be directly recorded within application using a FLIR camera. Other specialized hardware that is used during measurements (lamps, amplifiers, 3D scanners) can be controlled from within the application. The program has extensive processing, analysis and visualisation capabilities.

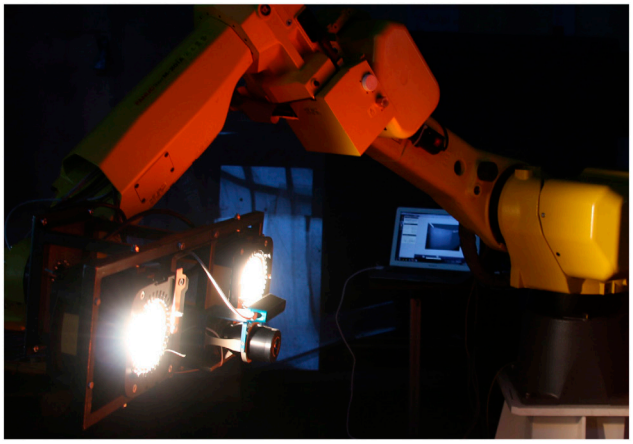

Figure 12. IR3D Analysis system mounted on robot, performing an automatic inspection of a part of a wind-turbine blade from both sides.

When IR3D Analysis results are viewed within application, it is possible to move to any desirable time during the whole analysis and observe the location of the measurement system (figure 13). The real-time renderer is deeply integrated with the rest of the software, which means all typical processing methods are available to the user. In active thermography an unprocessed image often does not reveal any information about the defects that may be present in the structure. It is regularly required to use advanced processing methods such as TSR or pulsed phase thermography (PPT) [42] to get information about the size and location of the defect. The proposed real-time rendering system allows to immediately see the updated infrared image on the geometrical representation of the inspected object.

Because the rendering process is performed on a GPU unit, it requires a fairly powerful computer equipped with CUDA graphics card to operate in real-time. One of the requirements of the method was to make it industry ready. This means, that the most important analysis results have to be easily viewable and accessible by normal engineers. Because of that, an additional representation—IR3D Snapshot—has been developed. IR3D Snapshot allows the user to permanently map the temperatures on the 3D model, as they are visible on the screen. IR3D snapshots are not rendered using ray-tracing algorithms and can be viewed almost on every existing machine.

5. Results

In order to verify the functionality of the new 3D thermography method, several analyses were performed on wind-turbine blades, planes and boats. Most interesting results were obtained during the diagnosis of a composite sea yacht. The

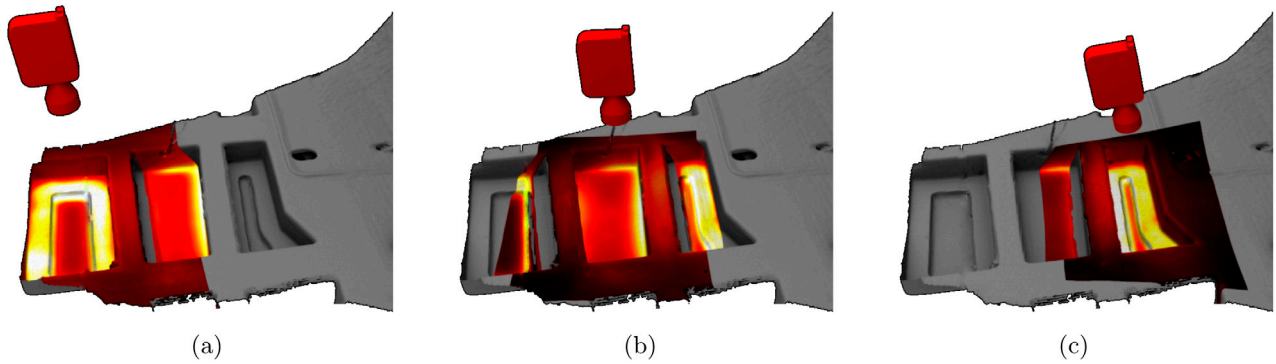

Figure 13. 3D visualisation of three consecutive measurement targeting different parts of the inspected structure. (a) First measurement. (b) Second measurement. (c) Third measurement.

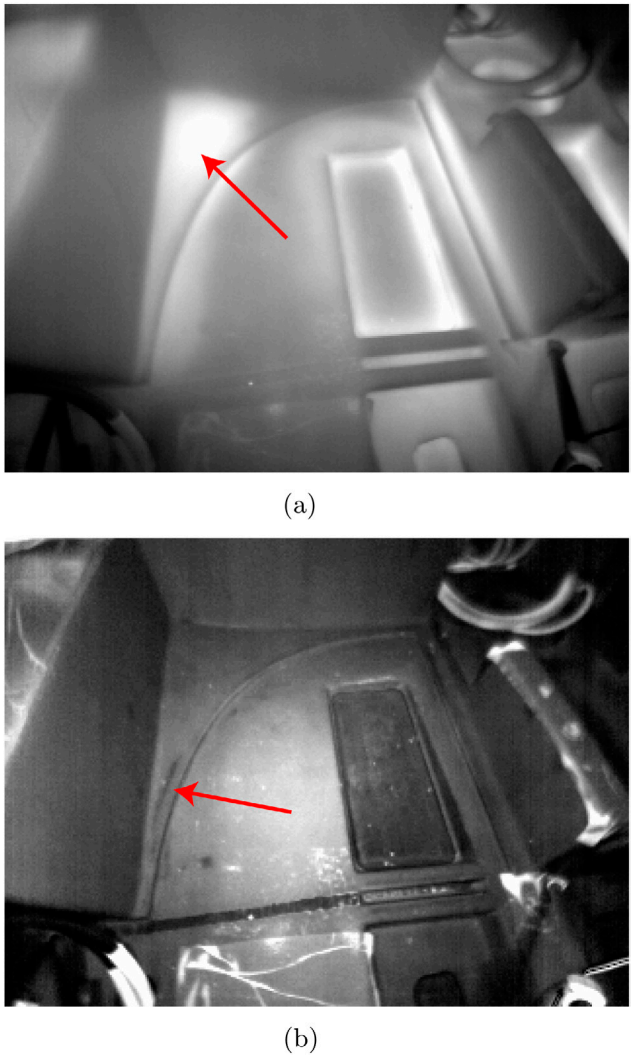

Figure 14. Passive and active thermography inspection of the boats hull. (a) Passive thermography. (b) Active thermography.

infrared inspection covered the boats hull, which is the body of the yacht below the deck. Both the hull and the deck are made out of composite materials. During the assembly, they are joined together with a thick layer of glue. The stiffness of the whole yacht is determined by the glued connection between the hull and the deck. After the assembly, it is important to

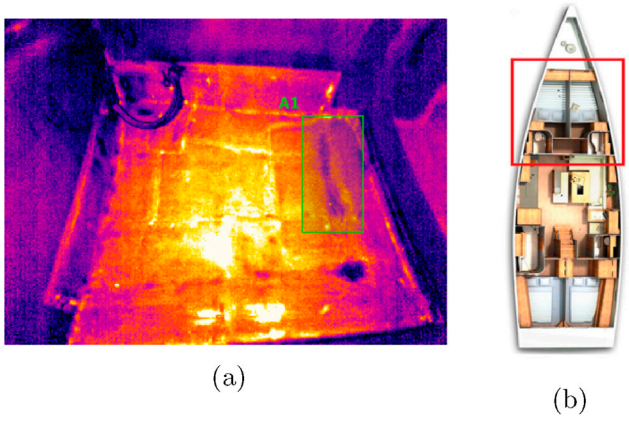

Figure 15. Discontinuity discovered on a front part of the boats hull. (a) Thermogram with defect. (b) Location.

verify the connection in most critical locations of the boat. Most of them are located in the center area of the hull.

The thermographic inspection of the hull consisted of two steps. The first task was to verify the glue distribution, as a non-uniform distribution may affect the boats stiffness. Additionally, the glued connection should be checked for the presence of air bubbles, which are not desirable and should be limited. The second task was verification of the quality of the composite itself. As the laminate is constructed by human workers, its quality is uneven throughout the hull. Additionally discontinuities may have been introduced in the composite material, when the parts were transported for assembly.

When diagnosing the boats hull, a unique measurement procedure has been used. The hull has been inspected directly after the assembly, when the glue still hasn't cooled down. Its average temperature was still 70 °C. A standard step pulse thermography analysis has been performed. Additionally, at the beginning of the measurement, a few sound frames were recorded, before the heating started. This way a single recorded thermogram consisted of two inspections:

- A passive thermography analysis, which is recorded before lamps start heating and allows to asses the glue distribution, while it is still hot,
- An active thermography analysis, which introduced external heating and inspects the quality of the laminate itself.

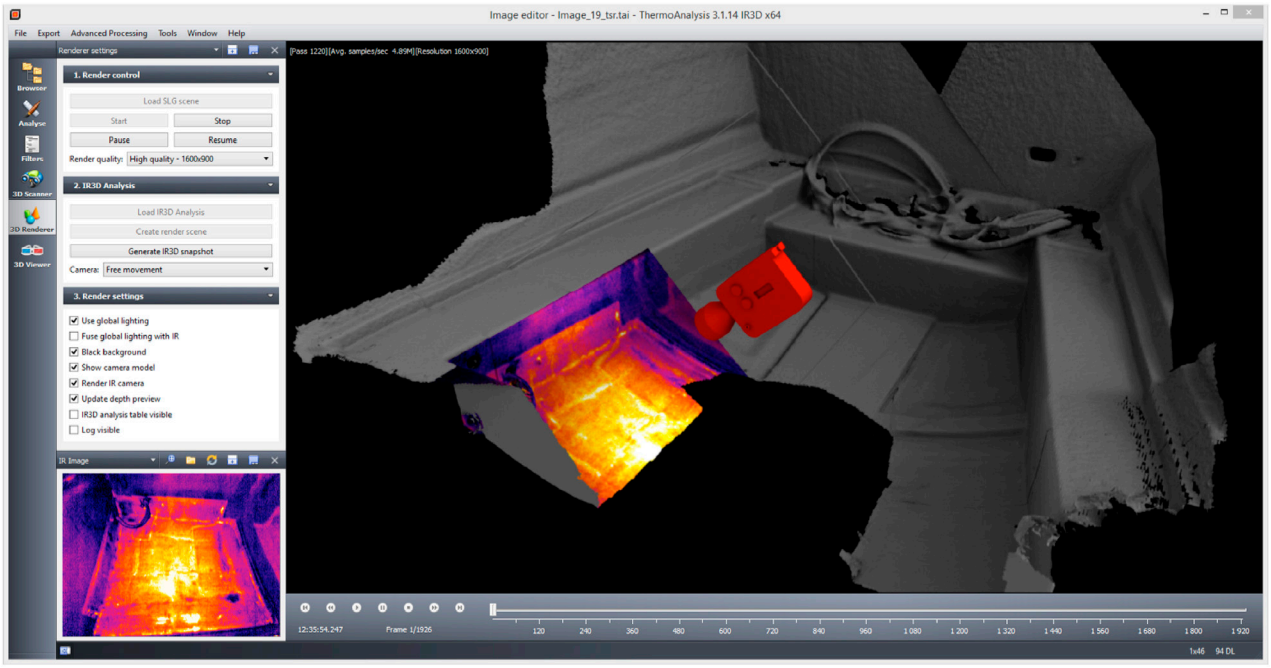

Figure 16. Visualisation of the results after IR3D Analysis of boats hull.

Figure 13 presented the results of a passive thermography inspection of the boats hull. The bright yellow colour corresponds to the distribution of hot glue. Three images were taken, each targeting different part of the boat. During post-processing the thermograms were mapped on the same 3D model. Because the model is constructed in metric units, it is possible to estimate the glue area coverage. This information can be used to estimate the quality of the connection.

The parameters of the long pulse thermography measurement have been selected in order to penetrate the thick laminate of the deck. Because the analysis was performed while the laminate was still very hot (although not as hot as the glue), the duration of the heating had to be extended to generate enough thermal contrast. Depending on the area of inspection, a single infrared measurement lasted from 40 to 250 s. The first few frames of every thermogram were recorded without any excitation applied, which allows to treat them as sound frames. They represent the thermal condition of the structure before the measurement.

Figure 14 presents exemplary results obtained from the diagnosis. The figure 14(a) shows the first frame of the acquired thermographic sequence, where the hot glue is presented by bright colours. The image allows us to assess the coverage of glue distribution. Figure 14(b) is a result obtained from the same thermographic file. The hot glue is no longer recognisable, but on the left side of the image a vertical discontinuity has been revealed. This is the result of processing the file using cold image subtraction combined with TSR. The basis of TSR method is to fit the temperature profiles of every pixel using a low-order polynomial function. This allows to greatly reduce the noise and improve the sensitivity of defect detection. The huge advantage of TSR processing is that it can be used to construct time derivative images, which allow to identify even smaller discontinuities.

Figure 15 displays another processed thermogram, which presents a non-uniform thermal response. The same processing methods were applied to the acquired thermographic sequence. The circular dark pattern, which can be observed in the bottom right part of the thermogram in figure 15(a), is a metal object which was mounted on top of the deck. The middle part of the thermogram has some bright reflections, which resulted from the inspected surface being uneven. However the large, vertical discontinuity marked as area A1 could not be identified, even after observing a normal vision image. After consultation with local technicians, a tap-testing verification was performed in the area. The area was determined to be a hollow space between the hull and the deck, and was later scheduled for repair.

The described measurement was performed in the front section of the boat, which estimated location is highlighted in figure 15. When viewing an infrared image, it is hard to identify the exact area that was diagnosed. Some thermal cameras contain an image fusion option, which allows to position the infrared image on top of a visible one. However, when the diagnosed surface does not contain many distinguishable features (e.g. it is only a planar surface) or there are many similar places on the diagnosed object, such picture in picture functionality may be insufficient. In order to fully define the measurements location and the hulls geometry, a 3D thermogram has been constructed, which can be observed in figure 16. By looking at the three-dimensional visualisation, it is possible to observe the surroundings, in which the measurement was taken and precisely specify the location of the delamination. Such information is very important, as it minimises the time and costs required to repair the inspected object.

The generated 3D model is defined in meters and contains the same dimensions as the inspected structure. This

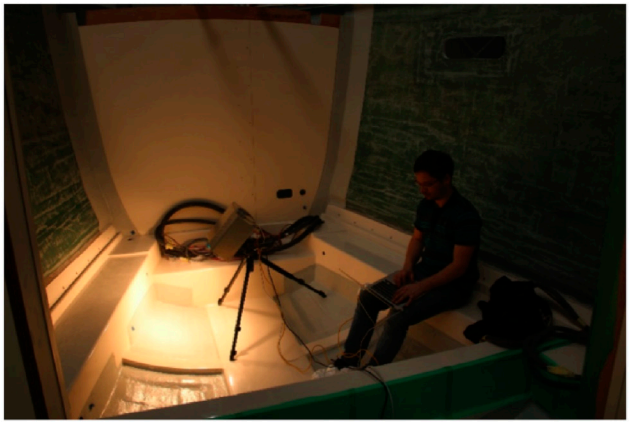

Figure 17. Inspection of a boats hull.

allows us to easily measure the size of defects, which are found on thermograms, without the need of any additional calibration. When performing a series of measurements on-site, it is often hard to keep constant distance to the inspected structure and place the camera perpendicularly (figure 17). Because of that, for every registered image a new scale calibration is required, in order to determine the pixel to millimetre ratio. By mapping the thermogram on 3D model, all dimensions can be easily extracted. This allows us to measure the discovered discontinuities directly on the model with millimetre precision, which helps in evaluation of their severity.

6. Conclusion

The authors presented a novel approach to 3D temperature mapping, which allows it to become a valuable tool in visualisation and localisation of defects in non-destructive testing methods, such as active thermography. Because of advanced cloud fusion algorithms, the method can be used even with the most common 3D scanners and still provide high quality results. The IR3D Analysis method is designed to be especially useful during diagnosis of large composite structures. It has been actively used both in laboratory and industrial environment. For the first time, the optimised algorithms allow for real-time temperature mapping.

Even though the presented method is fully working and has successfully been used in industrial applications, there are several aspects, which could be improved. The cloud fusion algorithm may sometimes lose itself, when the system is rapidly moved with high acceleration and not enough cloud points are registered. This can be improved by adding a gyroscope, which would track all the time the orientation of the camera and guide the fusion algorithm. Apart from the temperature data, it is possible to use the mounted RGB camera to additionally map coloured textured on the registered 3D model. Finally, in pulsed thermography measurement, it is possible to extract information about the depth of the registered defect. This information would allow to directly visualise the defect on generated 3D model, in the exact location as it appears in reality.

References

[1] Maldague X P V 2001 *Theory and Practice of Infrared Technology for Nondestructive Testing* (New York: Wiley) p 704

[2] Shepard S 2007 Flash thermography of aerospace composites *IV Conf. Panamericana de END Buenos Aires (October 2007)* vol **7**

[3] Grubišić I, Gjenero L, Lipić T, Sović I and Skala T 2011 Medical 3D thermography system *Periodicum Biologorum* **113** 401–6

[4] Wang C, Cho Y K and Gai M 2013 As-is 3D thermal modeling for existing building envelopes using a hybrid LIDAR system *J. Comput. Civ. Eng.* **27** 645–56

[5] Vollmer M and Mollman K 2010 *Infrared Thermal Imaging* (New York: Wiley)

[6] Czichos H 2013 *Handbook of Technical Diagnostics* (New York: Springer)

[7] Maldague X P V 2002 Introduction to NDT by active infrared thermography *Mater. Eval.* **60** 1060

[8] Milne J M and Reynolds W N 1985 The non-destructive evaluation of composites and other materials by thermal pulse video thermography *Proc. SPIE* **520** 119

[9] Meola C and Carlomagno G M 2004 Recent advances in the use of infrared thermography *Meas. Sci. Technol.* **15** R27

[10] Mix P E 2005 *Introduction to Nondestructive Testing: a Training Guide* (New York: Wiley) p 681

[11] Pieczonka L, Szwedo M and Uhl T 2011 Thermography of metallic and composite structures-review of applications *Diagn. Struct. Health Monit.* **2** 61–6

[12] Reynolds W N 1986 Thermographic methods applied to industrial materials *Can. J. Phys.* **64** 1150–4

[13] Ibarra-Castanedo C, Benítez H D, Maldague X P V and Bendada A 2007 Review of thermal-contrast-based signal processing techniques for the nondestructive testing and evaluation of materials by infrared thermography *Int. Workshop on Imaging NDE* vol **6**

[14] Shepard S 2001 *Proc. SPIE, Thermosense XXIII* pp 511–5

[15] Lazaros N, Sirakoulis G C and Gasteratos A 2008 *Int. J. Optomechatronics* **2** 435–62

[16] Westoby M J, Brasington J, Glasser N F, Hambrey M J and Reynolds J M 2012 *Geomorphology* **179** 300–14

[17] Linsen L 2001 Point cloud representation *Technical Report* Faculty of Informatics, University of Karlsruhe, Germany 1–18

[18] Weiss U and Biber P 2011 *Robot. Auton. Syst.* **59** 265–73

[19] Mankoff K D and Russo T A 2013 *Earth Surf. Process. Landf.* **38** 926–36

[20] Lagüela S, Armesto J, Arias P and Herráez J 2012 *Autom. Constr.* **27** 24–31

[21] Alba M I, Barazzetti L, Scaioni M, Rosina E and Previtali M 2011 *Remote Sens.* **3** 1847–70

[22] Borrmann D, Nüchter A, Dakulovic M, Maurovic I, Petrovic I, Osmankovic D and Velagic J 2012 The Project ThermalMapper—Thermal 3D mapping of indoor environments for saving energy *Proc. of the 10th Int. IFAC Symp. on Robot Control* vol **10** p 1

[23] Vidas S and Moghadam P 2013 *Energy Build.* **66** 445–60

[24] Vidas S, Moghadam P and Sridharan S 2015 *IEEE Sens. J.* **15** 1145–52

[25] Khoshelham K and Elberink S O 2012 *Sensors* **12** 1437–54

[26] Raposo C, Barreto J P and Nunes U 2013 Fast and accurate calibration of a kinect sensor *Proc.—2013 Int. Conf. on 3D Vision, 3DV* p 342

[27] Izadi S *et al* 2011 *Proc. of the 24th Annual ACM Symp. on User Interface Software and Technology* p 559

[28] Rusu R B and Cousins S 2011 3D is here: Point Cloud Library (PCL) *Proc.—IEEE Int. Conf. on Robotics and Automation (Shanghai)* pp 1–4

[29] Lorensen W E and Cline H E 1987 *ACM SIGGRAPH Computer Graphics* vol **21** p 163
[30] Rusinkiewicz S and Levoy M 2001 *Proc. 3rd Int. Conf. on 3D Digital Imaging and Modeling* pp 145–52
[31] Berger M, Alliez P, Tagliasacchi A, Seversky L M, Silva C T, Levine J A and Sharf A 2014 *Proc. of the Eurographics 2014, Eurographics STARS* pp 161–85
[32] Heredia F and Favier R 2012 Kinfu large scale in PCL www.pointclouds.org/blog/srcs/fheredia/ Accessed 17-01-2016
[33] Meister S, Izadi S and Kohli P 2012 When can we use KinectFusion for ground truth acquisition? *Proc. Workshop Color-Depth Camera Fusion Robot* pp 3–8
[34] Horn D R, Sugerman J, Houston M and Hanrahan P 2007 *Proc. of the 2007 Symp. on Interactive 3D Graphics and Games I3D 07* p 167
[35] LuxRender 2015 LuxRender GPL physically based renderer www.luxrender.net/ Accessed 11-01-2015
[36] Pharr M and Humphreys G 2010 *Physically Based Rendering, 2nd edition: from Theory To Implementation* (Burlington: Morgan Kaufmann Publishers Inc.)
[37] Claus D and Fitzgibbon A W 2005 *IEEE Computer Society Conf. on Computer Vision and Pattern Recognition* vol **1** pp 0–6
[38] Occipital I 2015 Structure sensor http://structure.io/ Accessed 01-11-2015
[39] Zhang Z 2000 *IEEE Trans. Pattern Anal. Mach. Intell.* **22** 1330–4
[40] Szwedo M and Hellstein P 2014 Qualitative diagnostics of wind-turbine blades inspection using active thermography *Int. Conf. on Quantitative Infrared Thermography (At Bordeaux, France)* (doi: 10.13140/2.1.1602.8488)
[41] MONIT SHM 2015 Thermoanalysis www.monitshm.pl/thermoanalysis Accessed 01-11-2015
[42] Maldague X and Marinetti S 1996 *J. Appl. Phys.* **79** 2694